

1 **Title:** Rapid transmission of coronavirus disease 2019 within a religious sect in South Korea: a
2 mathematical modeling study

3
4 **Authors:** Jong-Hoon Kim^{1*}, Hyojung Lee^{2,3+}, Yong Sul Won²⁺, Woo-Sik Son², and Justin Im¹

5 ¹International Vaccine Institute, Seoul, South Korea

6 ²National Institute for Mathematical Sciences, Daejeon, South Korea

7 ³Department of Statistics, Kyungpook National University, Daegu 41566, South Korea

8

9 ⁺Equal contribution

10 ^{*}Corresponding author:

11 Jong-Hoon Kim jonghoon.kim@ivi.int; kimfinale@gmail.com

12

13 **Abstract:** Rapid transmission of coronavirus disease 2019 (COVID-19) was observed in the
14 Shincheonji Church of Jesus, a religious sect in South Korea. The index case was confirmed on
15 February 18, 2020 in Daegu City, and within two weeks, 3,081 connected cases were identified.
16 Doubling times during the initial stages of the outbreak were less than 2 days. A stochastic model
17 fitted to the time series of confirmed cases suggests that the basic reproduction number (R_0) of
18 COVID-19 was 8.5 [95% credible interval (CrI): 6.3, 10.9] among the church members, whereas (R_0
19 = 1.9 [95% CrI: 0.4, 4.4]) in the rest of the population of Daegu City. The model also suggests that
20 there were 4 [95% CrI: 2, 11] undetected cases when the first case reported symptoms on February 7.
21 The Shincheonji Church cluster is likely to be emblematic of other outbreak-prone populations where
22 R_0 of COVID-19 is higher. Understanding and subsequently limiting the risk of transmission in such
23 high-risk places is key to effective control.

24 **NOTE:** This preprint reports new research that has not been certified by peer review and should not be used to guide clinical practice.

25 1. Introduction

26 Coronavirus disease 2019 (COVID-19) has become a global pandemic since it was first reported in
27 Wuhan, China in December 2019 with the name of novel coronavirus disease [1]. The causative agent,
28 severe acute respiratory syndrome coronavirus 2 (SARS-CoV-2), transmits mainly through human-
29 to-human contact [2], which can happen even during the infector is asymptomatic [3, 4]. Infection
30 with the virus causes diseases with varying degree of symptoms including death [5, 6]. Infection
31 mortality ratio is lowest among children aged between 5 and 9 years and increases loglinearly with
32 age [7].

33

34 One key characteristic of COVID-19 pandemic is that transmission events in high-risk settings such
35 as super-spreading events (SSEs) contribute to most transmissions [8, 9]. The risk of COVID-19
36 transmission is believed to high in places with high occupancy and poor ventilation [10]. One extreme
37 example is the outbreak in the Diamond Princess cruise ship, where 17% (619/3711) of the passengers
38 were infected from January 25 to February 20, 2020 [11]. Other examples include transmission events
39 in bars and wedding [8] in Hong Kong, nursing homes in U.S. [12], telemarketers working in group
40 in closed places [13] and fitness classes [14] in South Korea, and also religious gatherings, which we
41 describe below.

42

43 Explosive spread of COVID-19 was observed in the Shincheonji Church of Jesus (“Shincheonji”), a
44 religious sect in South Korea. The index case was confirmed on February 18, 2020 and within two
45 weeks, 3,081 connected cases were identified [15]. A simple calculation reveals that the outbreak size
46 doubled in less than every 2 days ($14/\log_2(3081) \approx 1.21$), which is smaller than doubling times
47 reported in the early stages of the COVID-19 outbreak in China (2.5 and 3.1 days in Hubei Province
48 and Hunan Province, respectively) [16], Spain (2.8 days) [17], the US (2.7 days) [18], and Korea (2.8
49 – 10.2 days) [19]. A total of 6,684 confirmed cases were reported in Daegu City as of March 31, 2020
50 of which 4,467 (66.8%) were Shincheonji members, representing close to half (47.9%, 4,467/9,334)
51 of the city’s total Shincheonji membership.

52

53 Previous studies highlighted that COVID-19 transmissions involve SSEs [20], which can play a key
54 role in sustained community transmissions [8, 9]. However, there have been no attempts to model the
55 dynamics of COVID-19 transmission within high-risk settings and their interaction with the general
56 community. In this study, we modeled the outbreak in the Shincheonji community while accounting
57 for its interaction with the rest of population. We used the stochastic model to account for the
58 stochastic nature of the transmission events. We used the model to explore the differences in the basic
59 reproduction number (R_0) between the high-risk setting and the general community, and quantify
60 uncertainties related to the initial conditions and dynamics of transmission under the dynamic
61 intervention programs.

62 **2. Materials and Methods**

63 *2.1 Background on the Shincheonji Church of Jesus*

64 Shincheonji was founded by Man-hee Lee in 1984 and has approximately 245,000 members including
65 30,000 foreigners [21]. At Shincheonji gatherings, worshipers used to sit close together on the floor
66 and facial coverings, such as glasses and face masks, are forbidden. Members were expected to attend
67 services despite illness [22]. The index case of the Daegu City outbreak was identified as a
68 Shincheonji member and some 1,000 people were reported to have attended worship together [23].
69 Further tracing of church members identified clustering in apartment complexes. Of 142 residents in
70 a particular Daegu apartment block, 94 (66%) were Shincheonji members of whom 46 (38.9%) tested
71 positive for the virus [24].

72 *2.2 Data*

73 Time series of patients confirmed with COVID-19 in Shincheonji community and the overall Daegu
74 City over the period of 19 February – 31 March 2020 was compiled based on the daily reports from
75 Korea Disease Control and Prevention Agency (KDCA) [15] (Figure 1). The reports provide the
76 number of cases confirmed with SARS-CoV 2 based on reverse transcription polymerase chain
77 reaction (RT-PCR) by category (Shincheonji or non-Shincheonji). We made some adjustments to the

78 existing data before we fit the model. First, in the beginning of the outbreak, KDCA provided both
79 daily and cumulative numbers of cases confirmed for SARS-CoV 2, which did not agree always. If
80 there is a discrepancy between these numbers, we prioritized cumulative numbers as this figure was
81 reported continuously throughout the outbreak. Second, data were missing for some days for the
82 number cases for Shincheonji members. We imputed missing values using the cubic spline method
83 (Figure S1 in the Supplementary Material).

84

85 2.3. Doubling time

86 The epidemic doubling time (T_d) represents the duration in which the cumulative incidence doubles.
87 Assuming exponential growth with a constant epidemic growth rate (r), the epidemic doubling time
88 can be calculated by the following equation [18, 25, 26]

$$T_d = \frac{\ln(2)}{r}. \quad (1)$$

89 Epidemic growth rate (r) may be estimated based on the data. For example, $r(t)$ can be estimated
90 by the following equation:

91

92

$$r(t) = \frac{\ln(C(t)) - \ln(C(t - \Delta t))}{\Delta t}, \quad (2)$$

93

94 where $C(t)$ indicates the cumulative number of infected people at time t and Δt is the duration over
95 which $r(t)$ is assumed to be constant. $r(t)$ can be calculated over the fixed time interval (e.g., 1 day
96 or 1 week) [27, 28] or variable time intervals (e.g., days on which the number of cases doubles,
97 quadruples, etc.) [19, 25]. We calculated doubling based on prior 7 days or 1 day from 18 February

98 to 5 March 2020, when the epidemic peaked and no further doubling of cumulative number of cases
99 occurred onward.

100

101 The basic reproduction number (R_0) is defined as the average number of secondary cases caused by
102 a single infected case in an entirely susceptible population and it provides sufficient information to
103 produce doubling times in the beginning of an outbreak. However, estimating R_0 requires additional
104 information such as generation time or developing a mechanistic model, and its estimates come with
105 higher degree of uncertainty [26]. Calculating doubling times requires fewer assumptions and also
106 allows us to compare our results with estimates from different settings where doubling times, but not
107 reproduction numbers, are available.

108 *2.4. Mechanistic model of COVID-19 transmission*

109 We developed a stochastic model of COVID-19 transmission within the Shincheonji community and
110 the overall population of Daegu City. The model includes six disease states: susceptible (S), exposed
111 but not infectious (E), pre-symptomatic but infectious (P), symptomatic and infectious (I),
112 asymptomatic but infectious (A), confirmed and isolated (C), and recovered (R). The model includes
113 two patches to model Shincheonji and non-Shincheonji people, separately. Transmission rates may
114 differ for each patch and person from one patch may infect people from the other patch. (Figure 2).

115

116 This modeling framework of mixing between two distinct sub-populations has been adopted in
117 previous works, ranging from sexually transmitted diseases [29] to vector-borne diseases such as
118 dengue [30], where formulations for mixing between patches vary. We adopted the formulation used

119 in the work on modeling transmission of cholera between hotspot and non-hotspot areas [31]. Mixing
120 between two sub-populations are defined by the 2×2 contact matrix,

121
$$C = \begin{pmatrix} c_{12} & c_{12} \\ c_{21} & c_{22} \end{pmatrix},$$

122 where c_{ij} indicates the fraction of time that individuals from patch i spends in patch j . Next, we
123 impose two conditions on the matrix C :

- 124 (i) Individuals must reside in either of the two patches, i.e., $c_{i1} + c_{i2} = 1$ for $i=1$
125 (Shincheonji) and 2 (non-Shincheonji).
- 126 (ii) The population in each patch remains constant, i.e., $c_{12}N_1 = c_{21}N_2$, where N_1 and
127 N_2 represent population size for patch 1 and 2, respectively.

128 The above conditions may transform the contact matrix C to the following form:

129

130
$$C = \begin{pmatrix} 1 - c_{12} & c_{12} \\ \frac{c_{12}N_1}{N_2} & 1 - \frac{c_{12}N_1}{N_2} \end{pmatrix}$$

131

132 containing only one unknown parameter c_{12} .

133

134 The force of infection for individuals from patch i at time t , $\lambda_i(t)$, is defined as follows:

$$\lambda_i(t) = \sum_j c_{ij} \beta_j \frac{\sum_k c_{kj} I_k(t)}{\sum_k c_{kj} N_k(t)}, \quad (3)$$

135 where β_j indicates local transmission rate in patch j and $I_k(t)$ indicates number of infectious
136 individuals from patch k .

137

138 The transitions between states are modeled using an explicit tau-leap algorithm [32] to account for
139 stochasticity of the infection transmission process. The number of susceptible people in patch i at
140 time $t + \Delta t$, $S_i(t + \Delta t)$, is written as follows:

141

$$S_i(t + \Delta t) = S_i(t) - Q_i^{SE}(t, t + \Delta t). \quad (4)$$

142 $Q_i^{SE}(t, t + \Delta t)$ represents the number of people who transit from state S to state E from t to $t + \Delta t$
143 in patch i and is a random variable with binomial distribution:

$$\text{Bin}(S_i(t), \Delta t \lambda_i(t)). \quad (5)$$

144 That is, it is represented as an integer varying between 0 and $S_i(t)$. For states from which more than
145 one potential transition exist (e.g., P to either A or I), multinomial distributions were applied. For
146 instance, the number of people transit from P to either I or A are given as follows:

$$\text{Multi}(P_i(t), \Delta t \pi), \quad (6)$$

147 where π is a vector given as

148

$$\left(\frac{1-f}{1/\delta - 1/\epsilon}, \frac{f}{1/\delta - 1/\epsilon} \right). \quad (7)$$

149

150 The first element of π indicates a probability of transition from P to I and the second element
151 indicates the probability of transition from P to A . The number of people in other states (i.e.,
152 E, A, I, C, R) at time t can be described similarly. The model was implemented in a combination of R

153 and C++ languages, in which the core transmission model part is expensive and was written in C++.

154 All the computer codes that generate the results in this paper are available on GitHub [33].

155

156 2.5. Modeling intervention program

157 To account for intensification of the intervention such as case isolation and contact tracing with
158 subsequent testing during the outbreak, we assumed case isolation rate (1 / mean time between
159 symptom onset and case isolation) and transmission rate of the infectious people per unit time change
160 over time. Specifically, we assumed that the case isolation rate, $\alpha(t)$, starts increasing on February
161 20 from the initial value of α^{init} when 4,474 out of 9,334 Shincheonji members were identified and
162 were asked to self-isolate. During model fitting, we let data suggest the duration of intervention, d
163 in day, which is the time required for the case isolation rate to reach its minimum, $\alpha(t) = \alpha^{\text{final}}$ for
164 $t > \text{February } 20 + d$. We assumed that the mean time between symptom onset and case isolation
165 linearly decreases over the intervention period d . In other words, $\alpha(t)$ is formulated as follows:

166

$$\alpha(t) = \begin{cases} 0, & \text{if } t < \text{Feb } 17 \\ \alpha^{\text{init}}, & \text{if } \text{Feb } 17 \leq t < \text{Feb } 20 \\ \alpha^{\text{init}} + (t - \text{Feb } 20)(\alpha^{\text{init}} - \alpha^{\text{final}})/d, & \text{if } \text{Feb } 20 \leq t < \text{Feb } 20 + d \\ \alpha^{\text{final}}, & \text{if } \text{Feb } 20 + d \leq t \end{cases} \quad (8)$$

167

168 where α^{final} is assumed to be 1 day based on the experiences in Busan City in Korea and $\alpha(t)$ is
169 assumed to be zero before February 17 when the index case was detected.

170

171 Similarly, transmission rate per unit time at time t , $\beta_i(t)$ for $i = 1$ (Shincheonji members), 2 (non-
172 Shincheonji people in Daegu City), is assumed to linearly decrease during the intervention period.

173

$$\beta_i(t) = \begin{cases} \beta_i^{\text{init}}, & \text{if } t < \text{Feb } 20 \\ \beta_i^{\text{init}} - (t - \text{Feb } 20)(\beta_i^{\text{init}} - \beta_i^{\text{final}})/d, & \text{if } \text{Feb } 20 \leq t < \text{Feb } 20 + d \\ \beta_i^{\text{final}}, & \text{if } \text{Feb } 20 + d \leq t \end{cases} \quad (9)$$

174 Here, β_i^{init} and β_i^{final} indicate the transmission rate per unit time before the intervention and after the
175 intervention measures fully take effect, respectively. They can be derived once $R_{0,i}$ and R^{final} are
176 given as:

$$\beta_i^{\text{init}} = \frac{R_{0,i}}{\frac{1}{\delta} - \frac{1}{\epsilon} + \frac{f}{\gamma + \alpha\rho} + \frac{1-f}{\gamma + \alpha}} \quad (10)$$

and

$$\beta_i^{\text{final}} = \frac{R^{\text{final}}}{\frac{1}{\delta} - \frac{1}{\epsilon} + \frac{f}{\gamma + \alpha\rho} + \frac{1-f}{\gamma + \alpha}} \quad (11)$$

177 2.6. Parameter estimation

178 Our model of COVID-19 transmission requires 15 parameters (Table 1). We divided the model
179 parameters into three classes depending on our belief on their relative certainty. The first class
180 includes parameters related to the natural history of infection and population size and we deemed that
181 available parameter estimates are reliable. For these parameters, we used their point estimates based
182 on analyses of data on COVID-19 transmissions in Korea or China. For the second class, which
183 includes parameters related to intervention programs, we used our best guesses based on supporting
184 evidence but still acknowledged their uncertainty. Therefore, we analyzed the models under various
185 assumptions on their values within some pre-specified ranges. Finally, we defined six parameters that
186 are critical for characterizing dynamics of COVID-19 transmission in Shincheonji members and non-
187 Shincheonji people. We estimated these parameters by fitting the model to daily confirmed COVID-
188 19 cases of Shincheonji members and non-Shincheonji people.

189

190 Estimation of parameters $\theta = (R_{0,1}, R_{0,2}, I_0, c_{12}, d, R^{\text{final}})$ was based on Approximate Bayesian
191 Computation Sequential Monte Carlo (ABC-SMC) [34]. The ABC is a method for approximating
192 posterior distributions given data D , $p(\theta|D)$, by accepting proposed parameter values when the
193 difference between simulated data D^* and D , $d(D, D^*)$, is smaller than tolerance ϵ :

194
$$p(\theta|D) \approx p(\theta|d(D, D^*) \leq \epsilon).$$

195 For our model, $d(D, D^*)$ is defined as the sum of the squared differences in daily confirmed cases
196 over the outbreak of duration T days, that is,

197
$$d_i(D, D^*) = \sum_{t=1}^T (D_t - D_t^*)^2,$$

198 for Shincheonji ($i = 1$) and non-Shincheonji ($i = 2$). Here, D_t and D_t^* represent observed daily
199 confirmed cases and model predicted values at time day t , respectively. ABC-SMC was designed to
200 increase efficiency of the ABC method and ABC is applied in a sequential manner by constructing
201 intermediate distributions, which converge to the posterior distribution. Tolerance ϵ is gradually
202 decreased and each intermediate distribution is obtained as a sample that is drawn with weights from
203 the previous distribution and then perturbed through a kernel $K(\theta|\theta^*)$. The kernel helps keep the
204 algorithm from being stuck in local optimum while maintaining the efficiency of the ABC-SMC
205 method. Minimally informative uniform distributions were used as prior distributions and estimation
206 procedure was repeated for ten different random seeds. The resulting distribution was summarized as
207 median, 50% credible intervals (CrI; interval between 25% and 75% percentiles) and 95% CrI
208 (interval between 2.5% and 97.5% percentiles). More details of the algorithm such as prior
209 distribution for each parameter, the number of steps, the tolerance values for each step, perturbation
210 kernel appear in the Supplementary Material.

211 **3. Results**

212 *3.1 Doubling time*

213 Over the period of February 18 – March 5, during which doubling of confirmed cases occurred 12
214 times, doubling times were <1 day in the beginning and increased subsequently with daily doubling
215 time presenting higher variability for both Shincheonji and non-Shincheonji values (Table 2).
216 Doubling times calculated over sliding one-week intervals remained shorter than 3 days for the most
217 part for both Sincheonji and non-Shincheonji population.

218 *3.2 Comparison between observations and the mechanistic model*

219 Our fitted model projects the trajectory of number of daily and cumulative confirmed cases in
220 Shincheonji and in the rest of the population of Daegu City (Figure 3(a)-(d)). The model correctly
221 projects the decreasing trends in both patches after reaching the peak on around March 3, 2020.
222 However, for the non-Shincheonji, daily new cases are underestimated toward the end of the outbreak.
223 R_0 were estimated to be quite different across two patches (Figure 3(e)). The local reproduction
224 number in the patch representing Shincheonji members, $R_{0,1}$, was estimated to be 8.54 [95% credible
225 interval (CrI): 6.30, 10.95] whereas the local reproduction number in the patch representing non-
226 Shincheonji members, $R_{0,2}$, was estimated to be 1.87 [95% CrI: 0.38, 4.40]. The time taken for the
227 intervention program to have exerted highest effect, d , is around 9.02 days [95% CrI: 7.85, 10.45],
228 which leads to both reduced transmission rate per unit time and reproduction numbers ($R^{\text{final}} = 0.34$
229 [95% CrI: 0.18, 0.53]). The model also suggests that there were infectious people already when the
230 first cases was symptomatic on February 7 ($I_0 = 4$ [95% CrI: 2, 11]). The proportion of time that a
231 person from Shincheonji members spends mixing with non-Shincheonji people, c_{12} , was estimate be
232 around 0.14 [95% CrI: 0.05, 0.22]. Posterior distribution of parameters based on 2,000 samples
233 obtained from 10 different random seeds and two-way correlations appear in Supplementary Material
234 (Figure S2).

235

236

237 4. Discussion

238 Rapid transmission of COVID-19 within the Shincheonji community is likely to have been facilitated
239 by high intensity contact between individuals gathering during services and in residential areas. Our
240 mathematical modeling analyses quantify the rapid spread of COVID-19 in Daegu City driven by a
241 community of Shincheonji members. The median R_0 among Shincheonji members ($R_{0,1}$) was 8.5,
242 which is over 4-fold higher than what was estimated for the rest of the population in Daegu City
243 ($R_{0,2}=1.9$). While the R_0 in the Shincheonji community is higher than estimates from most
244 transmission hotspots (e.g., in China [35-39] and Korea [40-43]), such high R_0 is not unusual in
245 particular considering that R_0 can be different depending on the local settings with varying contact
246 rates [44]. Studies do report that R_0 estimates of COVID-19 that are comparable or even higher than
247 our estimates for the Shincheonji community. During periods of intensive social contacts near the
248 Chinese New Year in China, R_0 was estimated to be 6 [45, 46]. Also, R_0 estimates were around 5
249 among those traveled from Wuhan and were subsequently confirmed in other countries [47], and
250 around 7 during the initial growth phase in the UK [48]. In an extreme setting such as the Diamond
251 Princess ship, much higher estimates ($R_0 = 14.8$) were reported [49]. Although the previous studies
252 that included data on the outbreak in Shincheonji community report smaller R_0 estimates [40, 42]
253 than our estimates, the difference might stem from that prior studies did not model the Shincheonji
254 community separately from the rest of the population and therefore measured the R_0 averaged across
255 sub-population that are highly heterogeneous.

256

257 Although estimated daily doubling times show some variability (e.g., 14 days on February 28 and
258 69.6 days on March 1 for the non-Shincheonji population), they are short overall, which indicates
259 rapid growth of the outbreak, and are compatible with estimates from other settings. Daily doubling
260 times were lower than one day in the beginning of the outbreak and this is similar to the estimates
261 from several regions in China [25]. The study by Shim *et al.* [19] used the dataset from Daegu City,
262 Korea including Shincheonji population produced the doubling time of 2.8 days [95% CI: 2.5, 4.0].
263 Our daily doubling time estimates averaged over the period of February 18 – March 5 is 2.9 days and
264 is consistent with the study. The period from February 18 to March 5 is likely to have been used in
265 the study by Shim *et al.* because the authors calculated the doubling times on the days when the
266 reported cases doubled and during the period of February 18 – March 5 the number of cases doubled
267 12 times and no further doubling occurred since then. The study by Lee *et al.* [50] used similar data,
268 but reported seemingly inconsistent findings, doubling time of 2.9 days for the first week and 3.4 over
269 the period around February 18 – March 4 considering that our estimate averaged over the first week
270 is 0.9 day. One likely reason for this difference is that Lee *et al.* calculated the doubling time using
271 the cumulative incidence estimated from a logistic model that used the initial value (i.e., number of
272 infected people on February 18) as a free parameter. Figure 2D from their study indicates that the
273 number of infected people on 18 February is much larger than 1 and this might have led to the higher
274 doubling time than our estimates. This may also explain why Lee *et al.* estimates for a similar period
275 (i.e., February 18 – March 5) is higher than our estimates and those by Shim *et al.* [19].
276

277 The relationship between the doubling time and the R_0 provides two insights on our inferences on
278 R_0 . For an *SEIR* model, there exists an algebraic formula that describes the inverse relationship
279 between initial epidemic growth rate and R_0 [51, 52]. This inverse relationship suggests that short
280 doubling times during the early phase of the epidemic we calculated using the growth rates are
281 consistent with high R_0 for Shincheonji we estimated using the stochastic dynamic transmission
282 model (Table S2 in the Supplementary Material). On the other hand, while doubling times may be
283 reduced and imply high R_0 for non-Shincheonji people as well, such short doubling times can arise
284 through mixing (i.e., positive c_{12}) with Shincheonji of high R_0 even if the R_0 for the non-
285 Shincheonji people are not as high.

286

287 Parameters around asymptomatic infections of COVID-19 are largely unknown [53] and we
288 [54]tested the sensitivity of our inferences to our assumptions on two parameters related to
289 asymptomatic infection, namely the proportion of asymptomatic infection, f , and relative rate of
290 isolation of asymptomatic people, ρ (Figure S3 in Supplementary Material). R_0 for Shincheonji
291 people, $R_{0,1}$, and the final reproduction number, R^{final} , showed a slight increase with increasing f
292 or decreasing ρ while other parameter estimates remain relatively constant. We also tested the
293 sensitivity of our parameter estimates to α^{final} , maximum rate of isolation near the end of the
294 outbreak. α^{final} showed an inverse relationship with other intervention-related parameters such as
295 duration of intervention d , and reproduction number at the end of the outbreak, R^{final} . Overall, while
296 there are some quantitative differences in our parameter estimates in response to the change in our
297 assumptions on fixed parameters, $R_{0,1}$ was always over 4-fold higher than $R_{0,2}$.

298

299 While the first case was confirmed on February 18 for the Shincheonji outbreak, it was later revealed
300 that the first case had symptoms on February 7 and even earlier transmission events were also
301 suspected [54, 55]. This finding is consistent with our model analyses, which suggest there were 4
302 [95% CrI: 2, 11] infectious people on February 7. These undetected cases are likely to have
303 contributed to the explosive outbreak in the Shincheonji community. Studies suggest that a substantial
304 fraction of all SARS-CoV-2 infections were undetected. For Korea, it was suggested that the number
305 of undetected cases may be larger than the number of detected cases [56]. A study suggests that >
306 80% of all infections were undocumented during the initial spread in China [57]. In France, over the
307 period of 7 weeks since 28 June 2020 after the first lockdown, it was estimated that around 93% of
308 all symptomatic cases were undetected initially and later around 69% of symptomatic cases were
309 undetected by the time when case ascertainment improved [58].

310

311 We have shown that SARS-CoV 2 has disproportionately affected a religious community generating
312 a large cluster of linked cases in Korea. Similar large clusters of cases in high-risk settings have been
313 observed in Korea and elsewhere. In Korea, many similar outbreaks in high-risk settings have been
314 reported in the news including the outbreak in a dance class [14] and a call center [13]. In Singapore,
315 a total of 247 cases were confirmed as of March 17, 2020 and six clusters including the spread in a
316 hotel and in a church accounted for 45.3% of the total cases [59]. In Hong Kong, 1,038 cases were
317 confirmed from January 23 to April 28, 2020 and among them, 51.3% of cases were associated with

318 large clusters. Such social settings as bars, restaurants, weddings, and religious sites appeared at
319 increased risk of large outbreaks [8].

320

321 One limitation of our analyses is that the model was fit to date of case confirmation because the date
322 of symptom onset, which is more closely related with the date of infection, was not available. The
323 daily number of confirmed cases can abruptly change depending on the intensity of intervention
324 measures, of which the dynamics may not be consistent with disease transmission process. This means
325 using the data on case confirmation under dynamics intervention measures is challenging. We tried
326 to mitigate this difficulty by incorporating the dynamics of intervention programs by assuming that
327 the start date and duration of enhanced case detection vary while the case detection rate increases
328 over time and let the data suggest the values for those parameters.

329

330 **5. Conclusions**

331 The potential for large variations in R_0 for COVID-19 has important implications for the design and
332 effectiveness of control strategies. The efficacy of components of intervention programs, such as
333 contact tracing and physical distancing, is dependent on various environmental and societal factors
334 (e.g., large gatherings, physical proximity, high risk behaviors such as singing, etc.) that influence the
335 transmissibility of disease. Our analyses provide important insights that in order to minimize the risk
336 of sudden outbreaks, efforts to identify and preempt high transmission scenarios will be key to
337 controlling the spread of the COVID-19. Understanding and subsequently limiting the risk of

338 transmission in high-risk places such as the Shincheonji Church cluster in Korea is key to effective
339 control of COVID-19 transmission.

340

341 **Funding:** This research was partly supported by Government-wide R&D Fund project for infectious
342 disease research (GFID), Republic of Korea (grant number: HG18C0088) and National Institute for
343 Mathematical Sciences (NIMS) grant funded by the Korean Government (NIMS-B21910000).

344

345 **Acknowledgments:** All authors acknowledge discussions with the members of the Research and
346 Development on Integrated Surveillance System Development for Early Warning of Infectious
347 Diseases of Korea.

348

349

350

351

352

353

354

355

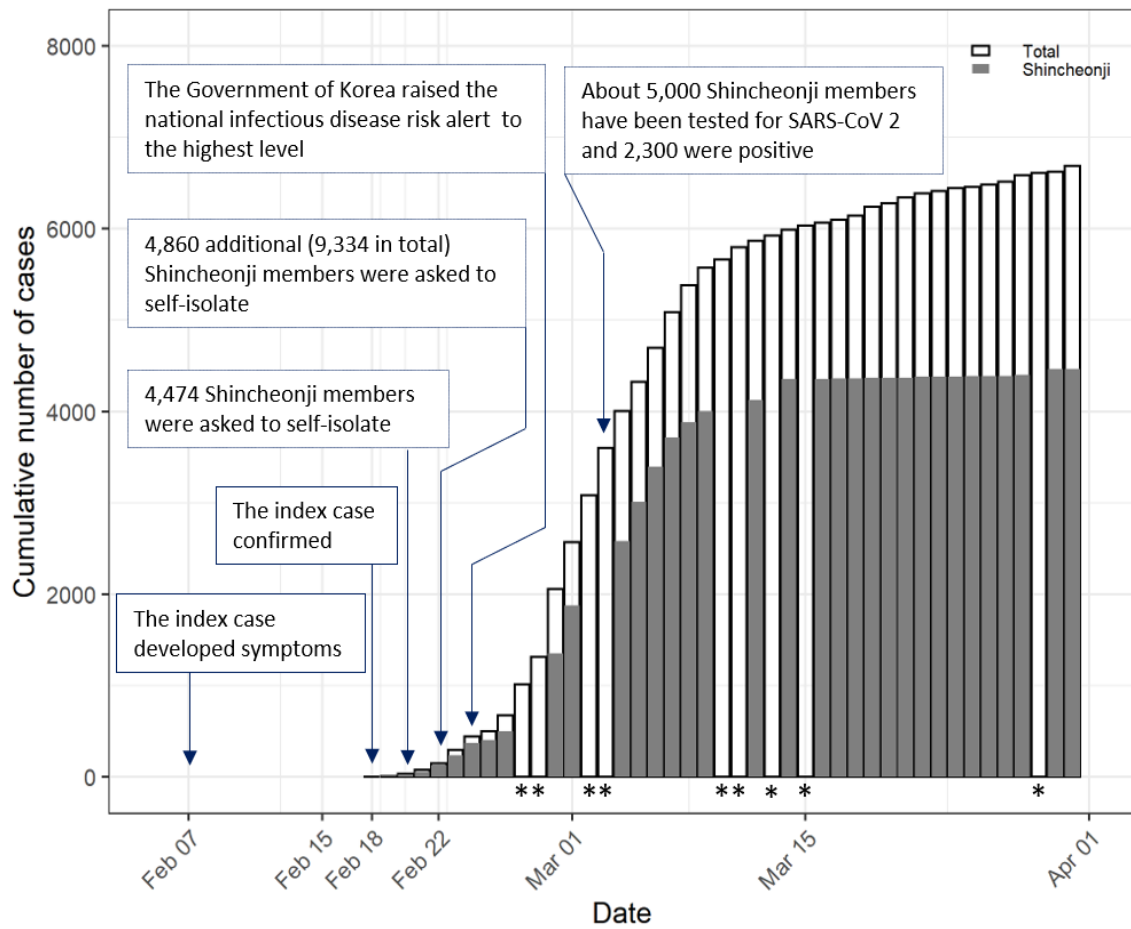
356

357

358

359 **Figure 1.** The daily number of confirmed COVID-19 cases from Daegu City, South Korea
 360 between 18 February and 31 March 2020. White bars represent overall cases from Daegu City
 361 including Shincheonji (Total) and grey bars represent cases associated with Shincheonji. Key
 362 events during the outbreak are described in the boxes. *Data on Shincheonji-associated cases are
 363 missing.

364



365

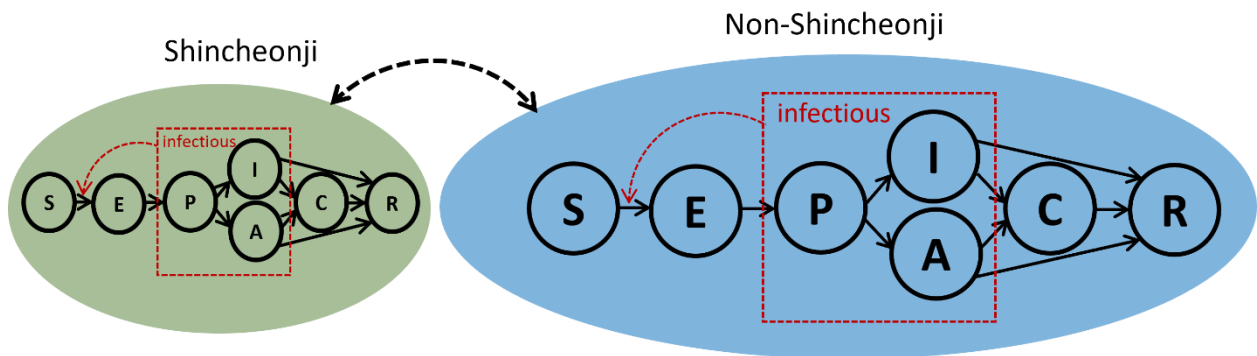
366

367

368

369

370 **Figure 2.** Schematic for the two-patch model. Circles with letters inside indicate compartments of
371 mutually exclusive states; susceptible (S), exposed but not infectious (E), pre-symptomatic but
372 infectious (P), symptomatic and infectious (I), asymptomatic but infectious (A), confirmed and
373 isolated (C), and recovered (R).
374



375

376

377

378

379

380

381

382

383

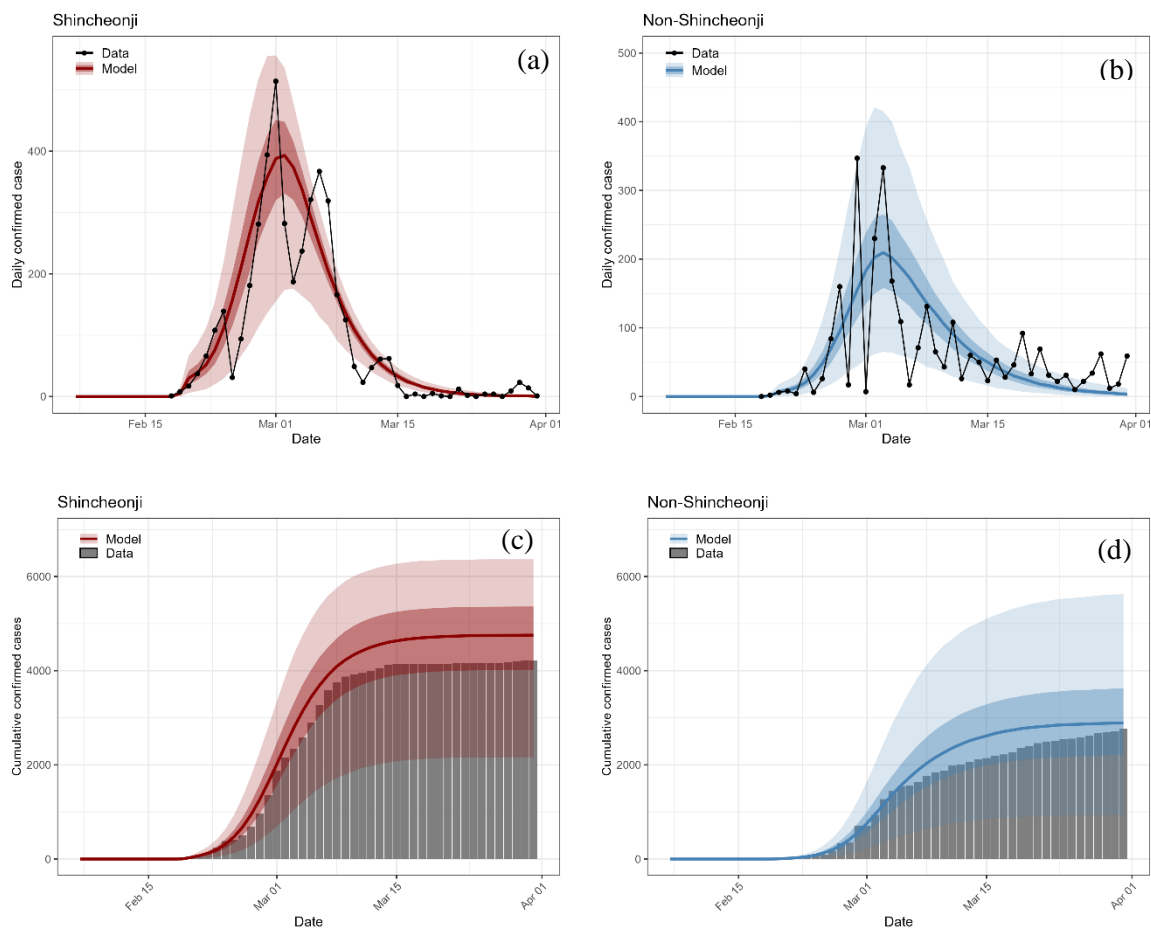
384

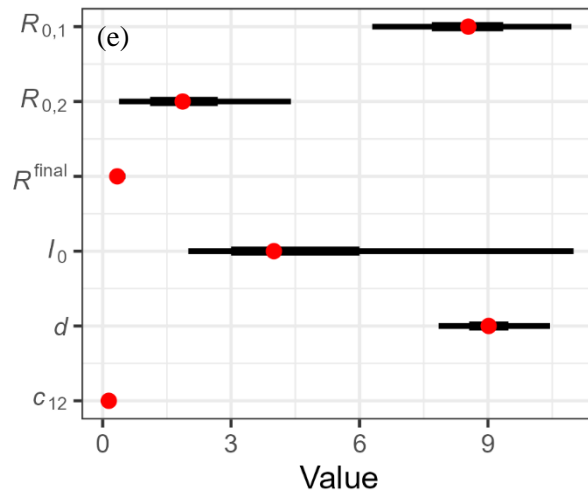
385

386

387

388 **Figure 3.** Parameter estimates and comparison between model outputs and data. Model outputs are
389 based on 2,000 simulation runs and presented with median (lines) with 50% (dark shading) and 95%
390 (light shading) percentiles. (a) and (b) represent daily number of confirmed COVID-19 cases from
391 the model and observations for Shincheonji and non-Shincheonji, respectively. (c) and (d) represent
392 cumulative confirmed cases from model outputs and data for Shincheonji and non-Shincheonji,
393 respectively. (e) shows posterior parameter estimates. Red dots represent the median, and thick and
394 thin bars represent 50% and 95% CrI of the posterior distribution for each parameter. Median for c_{12}
395 is 0.14 with its 50% CrI and 95% CrI being (0.11, 0.18) and (0.05, 0.22), respectively. Median for
396 R^{final} is 0.34 with its 50% CrI and 95% CrI being (0.28, 0.40) and (0.18, 0.53), respectively.
397





398

399

400

401

402

403

404

405

406

407

408

409

410

411

412

Table 1. Model parameters

Symbol	Parameter definition	Value	Source
<i>Parameters fixed throughout the simulation</i>			
N_2	Population size of the Daegu city excluding Shincheonji members	~2.5 million	[60]
N_1	Population size of the Shincheonji members	9,334	[15]
$1/\delta$	Mean time between infection and onset of symptoms (i.e., mean incubation period)	5.2 days	[1]
$1/\epsilon$	Mean time between infection and infectiousness (i.e., mean latent period)	3 days	[61]
$1/\gamma$	Mean time between symptom onset and recovery	14 days	Assumption
τ	Time when the intense intervention measures begin to be implemented	February 20	[15]
$1/\alpha^{\text{init}}$	Mean time between symptom onset and isolation of a patient in the beginning of the outbreak (i.e., time $t < \tau$)	4.3 days	[41]
<i>Parameters for which a range of values explored</i>			
ρ	Relate rate of isolation of asymptomatic cases to symptomatic cases. It is ρ before intervention measures, increases linearly and reaches 1 when the effect of intervention measures is highest	0.5 [0.1-0.9]	Assumption
f	Proportion of asymptomatic infections	0.306 [0.1 - 0.7]	[62]
$1/\alpha^{\text{final}}$	Mean time between symptom onset and isolation of a patient when the effect of intervention measures is highest	2 [1-3] days	Assumption ¹
<i>Estimated parameters</i>			
c_{12}	Proportion of time that individuals from Shincheonji (N_1) spends in non-Shincheonji (N_2). We assume $c_{12}N_1 = c_{21}N_2$ to keep the population size constant for each patch. See the Method section for details.		
I_0	Number of infectious people in Shincheonji on February 7		

$R_{0,1}$	Basic reproduction number in the patch representing the Shincheonji members
$R_{0,2}$	Basic reproduction number in the patch representing the non-Shincheonji people in Daegu City
d	Time it takes for the intervention measures to be fully implemented
R^{final}	Reproduction number (Shincheonji members and non-Shincheonji population in Daegu City) after the intervention measures are implemented. This is used to reflect the reduced transmission rate through case isolation, quarantine, and social distancing

¹The COVID-19 outbreak in Busan City, which occurred around the same time, indicate that delays from symptom onset to isolation were close to one day around the end of February when the outbreak started to flatten [63] (see data from Table S1 in the Supplementary Material).

Table 2. Doubling time during the Shincheonji outbreak during February 18 - March 5. On March 5, in total 4,443 cases (2,897 cases from Shincheonji and 1,546 cases from non-Shincheonji) were identified, which may indicate 12 times of doubling, and no subsequent doubling has happened.

Date	Cumulative incidence		Daily doubling time		Weekly rolling doubling time	
	Shincheonji	Non-Shincheonji	Shincheonji	Non-Shincheonji	Shincheonji	Non-Shincheonji
2020-02-18	1	0	-	-	-	-
2020-02-19	9	2	0.3	0.0	-	-
2020-02-20	26	8	0.7	0.5	-	-
2020-02-21	63	16	0.8	1.0	-	-
2020-02-22	129	20	1.0	3.1	-	-
2020-02-23	237	60	1.1	0.6	-	-
2020-02-24	376	66	1.5	7.3	-	-
2020-02-25	407	92	8.7	2.1	0.8	0.0
2020-02-26	501	176	3.3	1.1	1.2	1.1
2020-02-27	682*	335	2.2	1.1	1.5	1.3
2020-02-28	962*	352	2.0	14.0	1.8	1.6
2020-02-29	1356	699	2.0	1.0	2.1	1.4
2020-03-01	1870	706	2.2	69.6	2.3	2.0
2020-03-02	2152*	936	4.9	2.5	2.8	1.8
2020-03-03	2339*	1269	8.3	2.3	2.8	1.8
2020-03-04	2576	1437	7.2	5.6	3.0	2.3
2020-03-05	2897	1546	5.9	9.5	3.4	3.2

*Imputed numbers using a cubic spline method (see Methods and Supplementary Material)

- 1 1. Li, Q., et al., *Early Transmission Dynamics in Wuhan, China, of Novel Coronavirus-Infected Pneumonia*. N Engl J Med, 2020. **382**(13): p. 1199-1207.
- 2
- 3 2. Chan, J.F., et al., *A familial cluster of pneumonia associated with the 2019 novel coronavirus indicating person-*
4 *to-person transmission: a study of a family cluster*. Lancet, 2020. **395**(10223): p. 514-523.
- 5 3. Rothe, C., et al., *Transmission of 2019-nCoV Infection from an Asymptomatic Contact in Germany*. New
6 England Journal of Medicine, 2020. **382**(10): p. 970-971.
- 7 4. Yu, P., et al., *A Familial Cluster of Infection Associated With the 2019 Novel Coronavirus Indicating Possible*
8 *Person-to-Person Transmission During the Incubation Period*. J Infect Dis, 2020. **221**(11): p. 1757-1761.
- 9 5. Guan, W.J., et al., *Clinical Characteristics of Coronavirus Disease 2019 in China*. N Engl J Med, 2020. **382**(18):
10 p. 1708-1720.
- 11 6. Fu, L., et al., *Clinical characteristics of coronavirus disease 2019 (COVID-19) in China: A systematic review*
12 *and meta-analysis*. J Infect, 2020. **80**(6): p. 656-665.
- 13 7. O'Driscoll, M., et al., *Age-specific mortality and immunity patterns of SARS-CoV-2*. Nature, 2021. **590**(7844):
14 p. 140-145.
- 15 8. Adam, D.C., et al., *Clustering and superspreading potential of SARS-CoV-2 infections in Hong Kong*. Nat
16 Med, 2020. **26**(11): p. 1714-1719.
- 17 9. Lemieux, J.E., et al., *Phylogenetic analysis of SARS-CoV-2 in the Boston area highlights the role of recurrent*
18 *importation and superspreading events*. medRxiv, 2020: p. 2020.08.23.20178236.
- 19 10. Jones, N.R., et al., *Two metres or one: what is the evidence for physical distancing in covid-19?* BMJ, 2020. **370**:
20 p. m3223.
- 21 11. Russell, T.W., et al., *Estimating the infection and case fatality ratio for coronavirus disease (COVID-19) using*
22 *age-adjusted data from the outbreak on the Diamond Princess cruise ship, February 2020*. Euro Surveill, 2020.
23 **25**(12).
- 24 12. Chen, M.K., J.A. Chevalier, and E.F. Long, *Nursing home staff networks and COVID-19*. Proc Natl Acad
25 Sci U S A, 2021. **118**(1).
- 26 13. Park, S.Y., et al., *Coronavirus Disease Outbreak in Call Center, South Korea*. Emerg Infect Dis, 2020. **26**(8):
27 p. 1666-1670.
- 28 14. Jang, S., S.H. Han, and J.Y. Rhee, *Cluster of Coronavirus Disease Associated with Fitness Dance Classes, South*
29 *Korea*. Emerg Infect Dis, 2020. **26**(8): p. 1917-1920.
- 30 15. Korea Disease Control and Prevention Agency. *Press release*. 2020; Available from:
31 <https://www.cdc.go.kr/board/board.es?mid=a20501000000&bid=0015>.
- 32 16. Muniz-Rodriguez, K., et al., *Doubling Time of the COVID-19 Epidemic by Province, China*. Emerging
33 infectious diseases, 2020. **26**(8): p. 1912-1914.
- 34 17. Guirao, A., *The Covid-19 outbreak in Spain. A simple dynamics model, some lessons, and a theoretical framework*
35 *for control response*. Infectious Disease Modelling, 2020. **5**: p. 652-669.
- 36 18. Lurie, M.N., et al., *Coronavirus Disease 2019 Epidemic Doubling Time in the United States Before and During*
37 *Stay-at-Home Restrictions*. The Journal of Infectious Diseases, 2020. **222**(10): p. 1601-1606.
- 38 19. Shim, E., A. Tariq, and G. Chowell, *Spatial variability in reproduction number and doubling time across two*
39 *waves of the COVID-19 pandemic in South Korea, February to July, 2020*. Int J Infect Dis, 2020. **102**: p. 1-9.
- 40 20. Xu, X.K., et al., *Reconstruction of Transmission Pairs for Novel Coronavirus Disease 2019 (COVID-19) in*
41 *Mainland China: Estimation of Superspreading Events, Serial Interval, and Hazard of Infection*. 2020(1537-6591
42 (Electronic)).
- 43 21. Chung, E. and A. Hill, [DEBRIEFING] *What is the Shincheonji Church of Jesus and who are its members?*
44 *And more importantly, what are its links to the coronavirus?*, in Korea Joongang Daily. 2020.

- 45 22. Choe, S.-H., *Shadowy Church Is at Center of Coronavirus Outbreak in South Korea*, in *The New York Times*.
46 2020.
- 47 23. Yonhap, '*Shincheonji*' suspected as coronavirus hotbed, in *The Korea Times*. 2020.
- 48 24. Myung, M.-j., *Apartment block enters cohort isolation for the first time*, in *THE DONG-A ILBO*. 2020.
- 49 25. Muniz-Rodriguez, K., et al., *Doubling Time of the COVID-19 Epidemic by Province, China*. *Emerg Infect*
50 *Dis*, 2020. **26**(8): p. 1912.
- 51 26. Anderson, R.M., et al., *Reproduction number (R) and growth rate (r) of the COVID-19 epidemic in the UK: methods of estimation, data sources, causes of heterogeneity, and use as a guide in policy formulation*. The Royal
52 Society, 2020.
- 53 27. Ebell, M.H. and G. Bagwell-Adams, *Mandatory Social Distancing Associated With Increased Doubling Time: An Example Using Hyperlocal Data*. *American journal of preventive medicine*, 2020. **59**(1): p. 140-142.
- 54 28. Patel, S.B. and P. Patel, *Doubling Time and its Interpretation for COVID 19 Cases*. *Natl J Community Med*,
55 2020. **11**(1): p. 141-3.
- 56 29. Koopman, J., et al., *Sexual partner selectiveness effects on homosexual HIV transmission dynamics*. *J Acquir*
57 *Immune Defic Syndr* (1988), 1988. **1**(5): p. 486-504.
- 58 30. Lee, S. and C. Castillo-Chavez, *The role of residence times in two-patch dengue transmission dynamics and optimal strategies*. *J Theor Biol*, 2015. **374**: p. 152-64.
- 59 31. Azman, A.S. and J. Lessler, *Reactive vaccination in the presence of disease hotspots*. *Proc Biol Sci*, 2015.
60 **282**(1798): p. 20141341.
- 61 32. Gillespie, D.T., *Approximate accelerated stochastic simulation of chemically reacting systems*. *J Chem Phys*,
62 2001. **115**(4): p. 1716-1733.
- 63 33. Model codes. Available from: https://github.com/kimfinale/COVID_Shincheonji.
- 64 34. Minter, A. and R. Retkute, *Approximate Bayesian Computation for infectious disease modelling*. *Epidemics*,
65 2019. **29**: p. 100368.
- 66 35. Alimohamadi, Y., M. Taghdir, and M. Sepandi, *The Estimate of the Basic Reproduction Number for Novel*
67 *Coronavirus disease (COVID-19): A Systematic Review and Meta-Analysis*. *Korean J Prev Med*, 2020. **0**(0).
- 68 36. Wu, J.T., K. Leung, and G.M. Leung, *Nowcasting and forecasting the potential domestic and international spread of the 2019-nCoV outbreak originating in Wuhan, China: a modelling study*. *Lancet*, 2020.
- 69 37. Zhao, S., et al., *Preliminary estimation of the basic reproduction number of novel coronavirus (2019-nCoV) in*
70 *China, from 2019 to 2020: A data-driven analysis in the early phase of the outbreak*. *Int J Infect Dis*, 2020. **92**:
71 p. 214-217.
- 72 38. Riou, J. and C.L. Althaus, *Pattern of early human-to-human transmission of Wuhan 2019 novel coronavirus (2019-nCoV), December 2019 to January 2020*. *Euro Surveill*, 2020. **25**(4).
- 73 39. Imai, N., et al. *Report 3: Transmissibility of 2019-nCoV*. 2020.
- 74 40. Choi, S. and M. Ki, *Estimating the reproductive number and the outbreak size of COVID-19 in Korea*.
75 *Epidemiol Health*, 2020. **42**: p. e2020011.
- 76 41. Ki, M., *Epidemiologic characteristics of early cases with 2019 novel coronavirus (2019-nCoV) disease in Korea*.
77 2020(2092-7193) (Electronic).
- 78 42. Shim, E., et al., *Transmission potential and severity of COVID-19 in South Korea*. *Int J Infect Dis*, 2020. **93**: p.
79 339-344.
- 80 43. Bae, T.W., K.K. Kwon, and K.H. Kim, *Mass Infection Analysis of COVID-19 Using the SEIRD Model in*
81 *Daegu-Gyeongbuk of Korea from April to May, 2020*. *J Korean Med Sci*, 2020. **35**(34): p. e317.

- 87 44. Temime, L., et al., *A Conceptual Discussion About the Basic Reproduction Number of Severe Acute Respiratory*
88 *Syndrome Coronavirus 2 in Healthcare Settings*. Clinical Infectious Diseases, 2020.
- 89 45. Tang, B., et al., *Estimation of the Transmission Risk of the 2019-nCoV and Its Implication for Public Health*
90 *Interventions*. J Clin Med, 2020. **9**(2).
- 91 46. Sanche, S., et al., *The Novel Coronavirus, 2019-nCoV, is Highly Contagious and More Infectious Than Initially*
92 *Estimated*. medRxiv, 2020: p. 2020.02.07.20021154.
- 93 47. Zhao, Q., Y. Chen, and D.S. Small, *Analysis of the epidemic growth of the early 2019-nCoV outbreak using*
94 *internationally confirmed cases*. medRxiv, 2020: p. 2020.02.06.20020941.
- 95 48. Dropkin, G., *COVID-19 UK Lockdown Forecasts and R0*. Frontiers in Public Health, 2020. **8**(256).
- 96 49. Rocklöv, J., H. Sjödin, and A. Wilder-Smith, *COVID-19 outbreak on the Diamond Princess cruise ship:*
97 *estimating the epidemic potential and effectiveness of public health countermeasures*. J Travel Med, 2020. **27**(3).
- 98 50. Lee, W., et al., *COVID-19 in South Korea: epidemiological and spatiotemporal patterns of the spread and the*
99 *role of aggressive diagnostic tests in the early phase*. International Journal of Epidemiology, 2020. **49**(4): p.
100 1106-1116.
- 101 51. Ma, J., *Estimating epidemic exponential growth rate and basic reproduction number*. Infect Dis Model, 2020.
102 **5**: p. 129-141.
- 103 52. Ma, J., et al., *Estimating initial epidemic growth rates*. Bull Math Biol, 2014. **76**(1): p. 245-60.
- 104 53. Fox, S.J., et al., *The impact of asymptomatic COVID-19 infections on future pandemic waves*. medRxiv, 2020:
105 p. 2020.06.22.20137489.
- 106 54. *Serial interval*. Available from: https://en.wikipedia.org/wiki/Serial_interval.
- 107 55. Korea Disease Control and Prevention Agency, *Press release (February 22)*. 2020.
- 108 56. Lee, C., C. Apio, and T. Park, *Estimation of Undetected Asymptomatic COVID-19 Cases in South Korea Using*
109 *a Probabilistic Model*. Int J Environ Res Public Health, 2021. **18**(9).
- 110 57. Li, R., et al., *Substantial undocumented infection facilitates the rapid dissemination of novel coronavirus (SARS-*
111 *CoV-2)*. Science, 2020. **368**(6490): p. 489-493.
- 112 58. Pullano, G., et al., *Underdetection of cases of COVID-19 in France threatens epidemic control*. Nature, 2021.
113 **590**(7844): p. 134-139.
- 114 59. Tariq, A., et al., *Real-time monitoring the transmission potential of COVID-19 in Singapore, March 2020*. BMC
115 Med, 2020. **18**(1): p. 166.
- 116 60. Korean Statistical Information Service. 2019; Available from:
117 http://kosis.kr/statHtml/statHtml.do?orgId=101&tblId=INH_1B04005N_22.
- 118 61. He, X., et al., *Temporal dynamics in viral shedding and transmissibility of COVID-19*. Nature Medicine, 2020.
119 **26**(5): p. 672-675.
- 120 62. Kim, S.W., et al., *Clinical Characteristics and Outcomes of COVID-19 Cohort Patients in Daegu Metropolitan*
121 *City Outbreak in 2020*. J Korean Med Sci, 2021. **36**(1): p. e12.
- 122 63. Son, H., et al., *Epidemiological characteristics of and containment measures for COVID-19 in Busan, Korea*.
123 Epidemiol Health, 2020. **42**(0): p. e2020035-0.
- 124
- 125
- 126

Supplementary Material

Title: Rapid transmission of coronavirus disease 2019 within a religious sect in South Korea: a mathematical modeling study

Authors: Jong-Hoon Kim^{1*}, Hyojung Lee²⁺, Yong Sul Won²⁺, Woo-Sik Son², and Justin Im¹

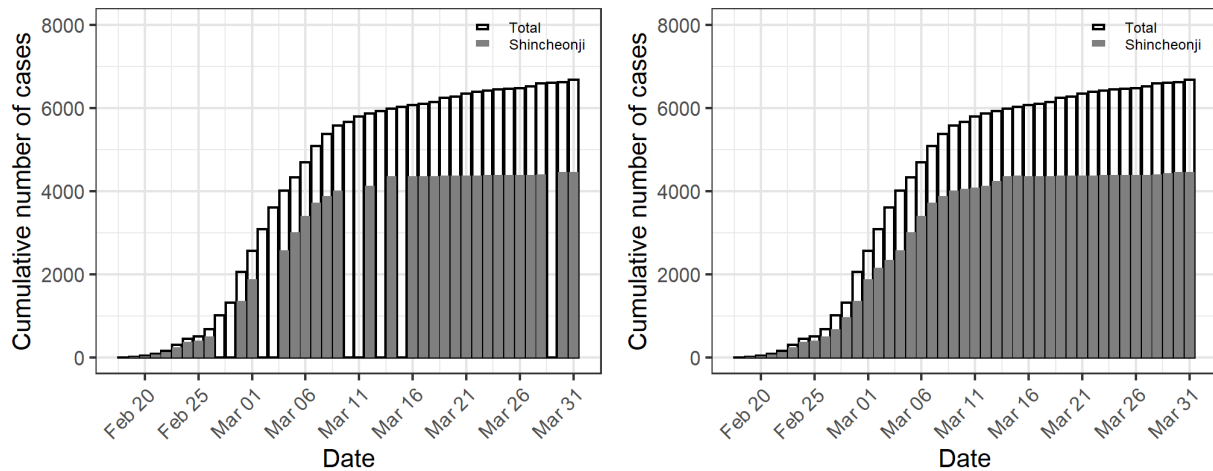
¹International Vaccine Institute, Seoul, South Korea

²National Institute for Mathematical Sciences, Daejeon, South Korea

Data source

Figure S1 shows the cumulative cases before and after imputation. We used the cubic spline method provided in the `imputeTS` package of R.

Figure S1. Cumulative number of cases in Shincheonji community and the overall Daegu before (left panel) and after imputation (right panel).



Model equations

The model is implemented using a tau-leap algorithm. The number of people who transit from state x to state y over the time interval from t to $t + \Delta t$ in patch i , $Q_i^{xy}(t, t + \Delta t)$, is defined as follows:

$$Q_i^{SE}(t, t + \Delta t) = \text{Bin}(S_i(t), \lambda_i(t)\Delta t),$$

where $\text{Bin}(n, p)$ represents binomial and with parameters n and p , respectively.

$$Q_i^{EP}(t, t + \Delta t) = \text{Bin}(E_i(t), \epsilon\Delta t),$$

$$Q_i^{Px}(t, t + \Delta t) = \text{Mult}(P_i(t), \pi),$$

where $\text{Multi}(n, \pi = \{\pi_1, \pi_2\})$ indicates multinomial distribution with parameters n and π . π is given as follows:

$$\pi = \left\{ \left(\frac{1}{1/\delta - 1/\epsilon} \right) (1 - f), \left(\frac{1}{1/\delta - 1/\epsilon} \right) f \right\}.$$

The first element of π indicates a probability for $x = I$ (i.e., transition from P to I) and the second element indicates the probability of transition from P to A ($x = A$). (1)

$$Q_i^{Ix}(t, t + \Delta t) = \text{Mult}(I_i(t), \pi),$$

$$\pi = \{\Delta t\alpha(t), \Delta t\gamma\},$$

The first element of π indicates a probability for $x = C$ (i.e., transition from I to C) and the second element indicates the probability of transition from I to R ($x = R$).

$$Q_i^{Ax}(t, t + \Delta t) = \text{Mult}(A_i(t), \pi),$$

$$\pi = \{\Delta t\alpha(t), \Delta t\gamma\}.$$

The first element of π indicates a probability for $x = C$ (i.e., transition from A to C) and the second element indicates the probability of transition from A to R ($x = R$).

The number of people in each state at time $t + \Delta t$ can be described using the terms defined above:

$$S_i(t + \Delta t) = S_i(t) - Q_i^{SE}(t, t + \Delta t),$$

$$E_i(t + \Delta t) = E_i(t) + Q_i^{SE}(t, t + \Delta t) - Q_i^{EP}(t, t + \Delta t),$$

$$P_i(t + \Delta t) = P_i(t) + Q_i^{EP}(t, t + \Delta t) - Q_i^{PA}(t, t + \Delta t) - Q_i^{PI}(t, t + \Delta t),$$

$$A_i(t + \Delta t) = A_i(t) + Q_i^{PA}(t, t + \Delta t) - Q_i^{AC}(t, t + \Delta t) - Q_i^{AR}(t, t + \Delta t),$$

$$I_i(t + \Delta t) = I_i(t) + Q_i^{PI}(t, t + \Delta t) - Q_i^{IC}(t, t + \Delta t) - Q_i^{IR}(t, t + \Delta t),$$

$$C_i(t + \Delta t) = C_i(t) + Q_i^{IC}(t, t + \Delta t) + Q_i^{AC}(t, t + \Delta t) - Q_i^{CR}(t, t + \Delta t),$$

$$R_i(t + \Delta t) = R_i(t) + Q_i^{AR}(t, t + \Delta t) + Q_i^{IR}(t, t + \Delta t) + Q_i^{CR}(t, t + \Delta t).$$

The model comprises two sets of above equations that describe two patches (i.e., a community of Shincheonji members and the non-Shincheonji people in Daegu City) and these equations are linked through the force of infection function, $\lambda(t)$, which is defined in the main text.

Table S1. Delay from onset of symptoms to isolation during the COVID-19 outbreak in Busan City, Korea.

Date	Median	Mean	Number of cases
2/6/2020	17.0	17.0	1
2/16/2020	8.0	8.0	1
2/17/2020	5.5	5.5	2
2/19/2020	4.0	3.7	7
2/20/2020	2.5	2.6	8
2/21/2020	1.5	2.2	6
2/22/2020	1.0	2.0	9
2/23/2020	2.0	1.8	4
2/24/2020	0.0	0.7	3
2/25/2020	1.5	1.5	2
2/26/2020	1.5	1.8	4
2/27/2020	1.0	2.0	3
2/28/2020	3.0	2.3	3
2/29/2020	6.0	6.0	2
3/1/2020	2.0	2.0	1
3/2/2020	3.0	3.0	1
3/4/2020	3.0	3.0	1
3/6/2020	8.0	8.0	1
3/9/2020	3.0	3.0	2
3/12/2020	1.0	1.0	1
4/8/2020	10.0	10.0	1
5/6/2020	3.5	3.5	2
5/10/2020	2.0	2.0	1
5/27/2020	2.0	2.0	1

*Number of isolated cases

Model fitting

A pseudocode for Approximate Bayesian Computation Sequential Monte Carlo (ABC-SMC) is presented below adopting what was presented in the previous study (Minter and Retkute, 2019):

1. Set the number of generations G and the number of particles N

2. Set the tolerance schedule $\epsilon_1 < \epsilon_2 < \epsilon_3 < \dots < \epsilon_G$ and set the generation indicator $g = 1$
3. Set the particle indicator $i = 1$
4. If $g = 1$, sample θ^{**} from the prior distribution $p(\theta)$. If $g > 1$, sample θ^* from the previous generation $\{\theta_{g-1}\}$ with weights $\{w_{g-1}\}$ and perturb the particle to obtain $\theta^{**} \sim K(\theta|\theta^*)$
5. If $p(\theta^{**}) = 0$, return to Step 4.
6. Generate n data sets D_j^{**} from the model using θ^{**} and calculate

$$\hat{p}(D|D^{**}) = \frac{1}{n} \sum_{j=1}^n 1(d(D, D_j^{**}) \leq \epsilon_g).$$

7. If $\hat{p}(D|D^{**}) = 0$, return to Step 4
8. Set $\theta_g^{(i)} = \theta^{**}$ and calculate the corresponding weight of the accepted particle i

$$w_g^{(i)} = \begin{cases} \hat{p}(D|D^{**})p(\theta^{**}), & \text{if } g = 1 \\ \frac{\hat{p}(D|D^{**})p(\theta^{**})}{\left(\sum_{j=1}^N w_{g-1}^{(j)} K(\theta_g^{(i)}|\theta_{g-1}^{(j)})\right)}, & \text{if } g > 1 \end{cases}$$

9. If $i < N$, increment $i = i + 1$ and go to step 4.
10. Normalize the weights so that $\sum_{i=1}^N w_g^{(i)} = 1$
11. If $g < G$, set $g = g + 1$, go to step 3

$K(\theta|\theta^*)$ was assumed to follow a multivariate normal distribution that was truncated to give only positive values. Twenty generations (i.e., $G = 20$) were used with the following tolerance for Shincheonji ($\epsilon_{1..G}^1$) and non-Shincheonji ($\epsilon_{1..G}^2$):

Initial tolerance values ϵ_1^s were set as

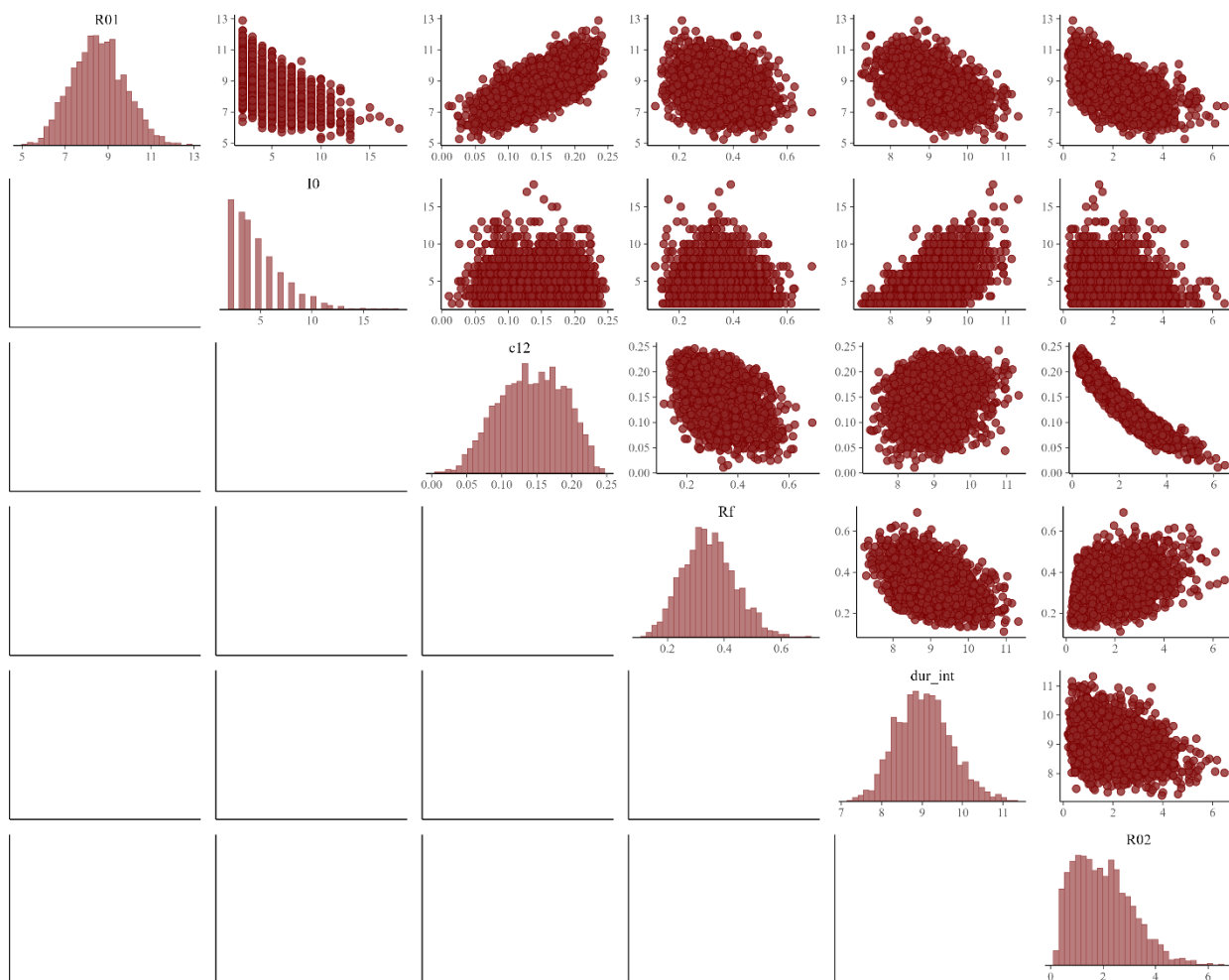
$$\sqrt{\sum_{j=1}^n (2 * y_{s,j})^2},$$

where y_j represent incidence of confirmed case on day j for Shincheonji ($s = 1$) and non-Shincheonji ($s = 2$), respectively. $\epsilon_{2..20}^s$ values were determined by setting the minimum values, ϵ_{20}^s , as $0.06 \times \epsilon_1^s$ and dividing 20 equidistance pieces. Finally, final two value were manually adjusted to provide good fit between data and the model predictions through trial and error. Below are actual values used but were rounded for presentation.

$$\epsilon_{1..G}^1 = \{2140, 2035, 1928, 1823, 1717, 1611, 1505, 1399, 1293, 1187, 1081, 975, 869, 764, 658, 552, 446, 340, 290, 250\}, \epsilon_{1..G}^2 = \{1325, 1260, 1194, 1129, 1063, 998, 932, 867, 801, 736, 670, 604, 539, 473, 408, 342, 277, 211, 190, 180\}.$$

Prior distributions for the parameters $\theta = (R_{0,1}, R_{0,2}, I_0, c_{12}, d, R^{\text{final}})$ were defined as uniform distribution as follows: $R_{0,1} \sim U(1, 20)$, $R_{0,2} \sim U(1, 20)$, $I_0 \sim U(1, 20)$, $c_{12} \sim U(0.000001, 1)$, $d \sim U(1, 30)$, $R^{\text{final}} \sim U(1, 20)$.

Figure S2. Posterior distribution of model parameters ($n=2000$). For each of 10 random seeds, 200 samples were generated.



Growth rate r and basic reproduction number R_0

For the differential equation-based *SIR* model, the initial (*i.e.*, the entire population is susceptible) epidemic growth rate r^* can be given as $\beta - \gamma$, (Ma, 2020) where β and γ represent transmission rate and recovery rate, respectively, as we defined in our model. Similarly, for a differential equation-based *SEIR* model r^* is given as below (Ma, 2020; Ma et al., 2014):

$$r^* = \frac{1}{2} \left[-(\epsilon + \gamma) + \sqrt{(\epsilon - \gamma)^2 + 4\beta\epsilon} \right],$$

where ϵ represent the rate at which the exposed individuals become infectious (*i.e.*, $\frac{1}{\epsilon}$ = mean latent period) as we defined in the main text. The above equation gives β and therefore R_0 for given r^* , γ , ϵ . Assuming $r^* = r$, which is the growth rate we calculated in the main text, we can see to what value of R_0 the doubling times we calculated in the main text are translated and qualitatively see if R_0 estimates from the current study are reasonable.

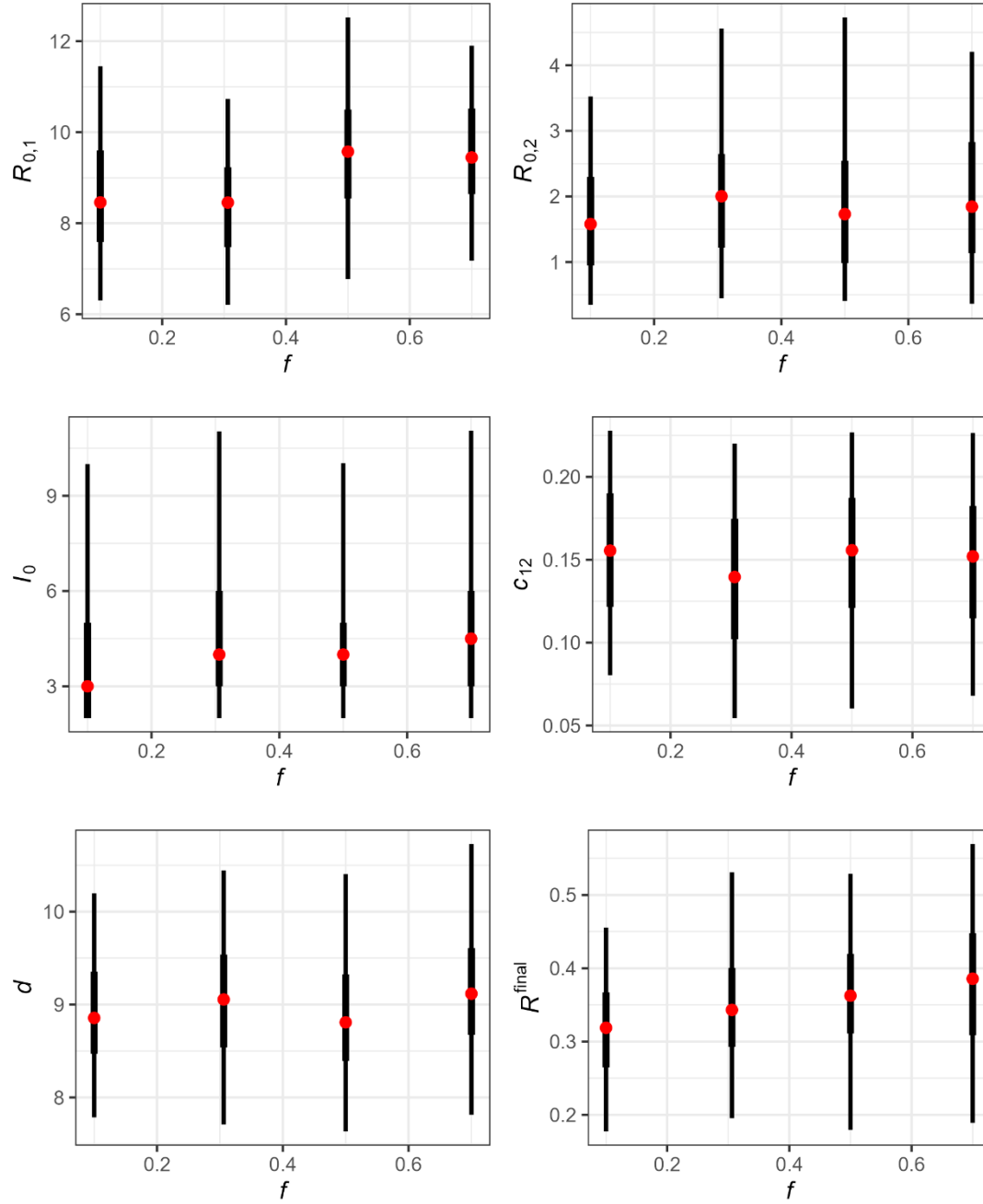
Table S2. Basic reproduction number, R_0 , calculated by assuming the empirical daily or weekly growth rate r is the same as the r^* calculated for the SEIR model.

Date	* R_0 calculated from the daily doubling time		R_0 calculated from the weekly rolling doubling time	
	Shincheonji	Non-Shincheonji	Shincheonji	Non-Shincheonji
2020-02-18	-	-	-	-
2020-02-19	127.0	-	-	-
2020-02-20	29.5	51.6	-	-
2020-02-21	23.9	17.0	-	-
2020-02-22	17.0	4.1	-	-
2020-02-23	14.7	38.0	-	-
2020-02-24	9.6	2.1	-	-
2020-02-25	1.9	6.3	23.9	
2020-02-26	3.9	14.7	13.0	14.7
2020-02-27	5.9	14.7	9.6	11.6
2020-02-28	6.6	1.5	7.5	8.8
2020-02-29	6.6	17.0	6.3	10.5
2020-03-01	5.9	1.1	5.6	6.6
2020-03-02	2.7	5.1	4.5	7.5
2020-03-03	1.9	5.6	4.5	7.5

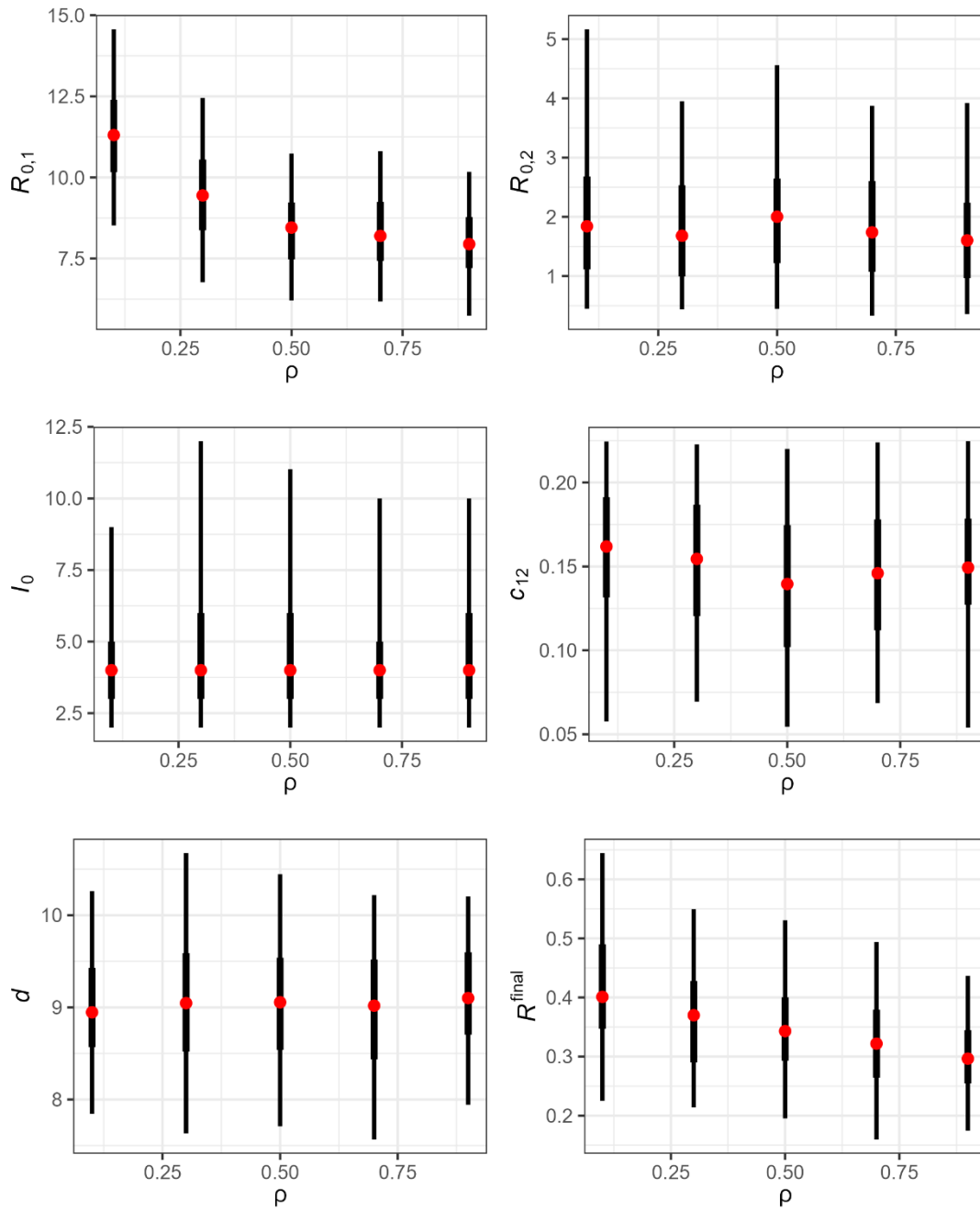
2020-03-04	2.1	2.5	4.2	5.6
2020-03-05	2.4	1.8	3.7	4.0

Figure S3. Sensitivity of our parameter estimates to simplifying assumption of three selected parameters

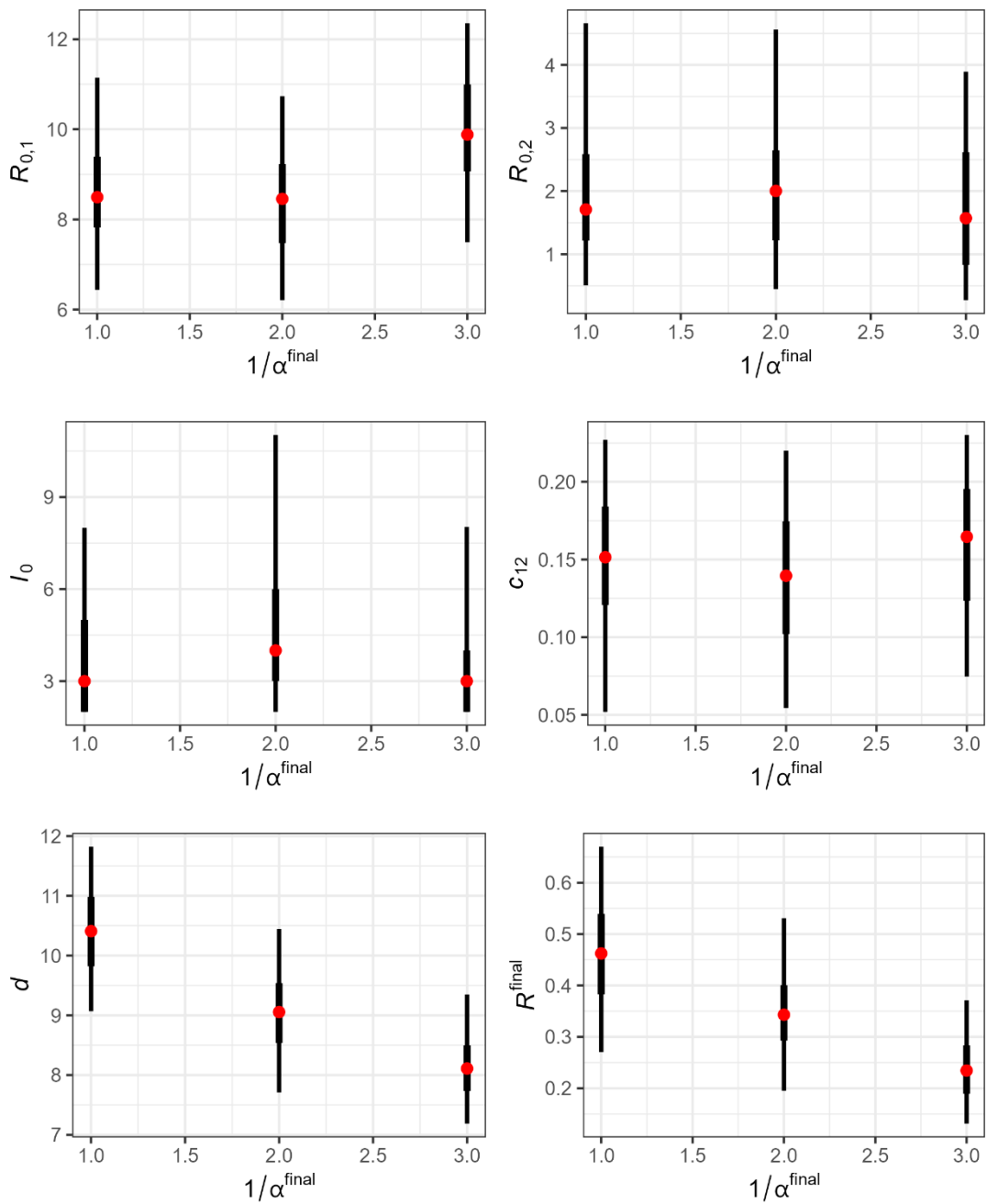
1) Fraction of asymptomatic infection f



2) Relative rate ρ of isolation of asymptomatic patients compared to the symptomatic patients before the intervention.



3) Time from symptom onset to isolation during the peak of the intervention, $1/\alpha^{\text{final}}$



References

- Ma, J., 2020. Estimating epidemic exponential growth rate and basic reproduction number. *Infect Dis Model* 5, 129-141.
- Ma, J., Dushoff, J., Bolker, B.M., Earn, D.J., 2014. Estimating initial epidemic growth rates. *Bull Math Biol* 76, 245-260.

Minter, A., Retkute, R., 2019. Approximate Bayesian Computation for infectious disease modelling. *Epidemics* 29, 100368.